An optical pump-probe technique for measuring the thermal conductivity of liquids

Cite as: Rev. Sci. Instrum. **79**, 064902 (2008); https://doi.org/10.1063/1.2937458
Submitted: 18 March 2008 . Accepted: 06 May 2008 . Published Online: 03 June 2008

Aaron Schmidt, Matteo Chiesa, Xiaoyuan Chen, and Gang Chen

An optical pump-probe technique for measuring the thermal conductivity of liquids

Aaron Schmidt,[a] Matteo Chiesa, Xiaoyuan Chen, and Gang Chen
Department of Mechanical Engineering, Massachussets Institute of Technology, Cambridge, Massachusetts 02139, USA

(Received 18 March 2008; accepted 6 May 2008; published online 3 June 2008)

We present a pump-probe optical technique for measuring the thermal conductivity of liquids. The technique uses a reflective geometry which does not depend on the optical properties of the liquid and requires as little as a single droplet to produce a result. An analytical solution is given for bidirectional heat flow in layered media, including the effects of radial heat flow from coaxial Gaussian laser spots, thermal interface resistances, and the accumulation of multiple laser pulses. In addition, several experimental improvements over previous pump-probe configurations are described, resulting in an improved signal to noise ratio and smaller errors at long stage delay times. The technique is applied to a range of liquids and solids. Results are in good agreement with literature values. © *2008 American Institute of Physics.* [DOI: 10.1063/1.2937458]

I. INTRODUCTION

Ultrafast lasers have been used to study thermal transport in a wide variety of situations, including electron-phonon coupling in metals,[1,2] the thermal conductivity of thin films and bulk materials,[3,4] the thermal conductance of solid-solid[5,6] and solid-liquid interfaces,[7,8] and thermal diffusion in bulk liquids.[9] Almost all of these experiments are variations on a pump-probe technique, in which a pump pulse is used to excite the sample, changing the optical properties, and a second time-delayed probe pulse measures the change. Typically, the data are compared to a model of the system, and the unknown properties of interest are adjusted to minimize the error between the model and the data.

In this paper, we present a convenient pump-probe method for measuring the thermal conductivity of liquids. The principle is simple: liquid is placed on a glass substrate coated with a thin film of metal. The laser impinges on the metal through the glass, and the cooling of the metal film is used to deduce the thermal conductivity of the adjacent liquid. Our apparatus incorporates several improvements over previously described systems, including a frequency-doubled pump beam to minimize noise from scattered light, a coaxial geometry for simplified alignment, and a beam expander to minimize probe divergence at long delay times. These improvements are relevant to the measurement of the properties of solids as well as liquids and are described in Sec. II. An analytical solution for the heat flow in our setup is obtained by extending the work of Capinski and Maris[10] and Cahill[11] to account for bidirectional heat flow. This is done in Sec. III.

Our approach has unique advantages over other methods for measuring the thermal conductivity of liquids. Only a few microliters of liquid (often a single droplet) are needed to obtain a reliable measurement. This is far less than the volume needed for the standard hotwire method developed by Nagasaka and Nagashima,[12] and at such small volumes the effects of convection are eliminated. Moreover, because there is no direct interaction between the laser light and the liquid, there are no restrictions on its optical properties. This is an advantage over transient grating methods which rely on thermally induced changes in the optical properties of the liquid to obtain thermal diffusivity.[9]

We have applied our technique to liquids spanning the range of commonly encountered thermal conductivities, from 0.05 W/m K (FC-72) to 0.6 W/m K (water) and have found good agreement with literature values. In addition, we successfully applied the technique to malleable solids including silicone grease and hardened epoxy.

II. EXPERIMENTAL SETUP

A schematic containing the essential features of our pump-probe system is shown in Fig. 1. A Ti:sapphire laser emits a train of 150 fs pulses at a repetition rate of 80.7 MHz. The center wavelength is 800 nm and the power per pulse is roughly 20 nJ. The main beam is divided into pump and probe beams with a polarizing beam splitter. The probe beam is expanded with a pair of lenses from a $1/e^2$ diameter of $\sim 2-8$ mm, and its optical path is adjusted up to 2.1 m (7 ns) with a double-pass delay stage.

The purpose of the beam expander is to minimize divergence of the probe beam at long delay times. A perfectly columnated beam with $1/e^2$ radius w_0 will diverge according to[13]

$$w = w_0\left[1 + \left(\frac{\lambda z}{\pi w_0^2}\right)^2\right]^{1/2}. \quad (1)$$

Here w is the $1/e^2$ beam radius, λ is the wavelength, and z is the propagation distance. Without expansion, our beam radius would increase by $\sim 12\%$ at maximum delay, translating roughly into a corresponding increase in focused spot size. After expansion, Eq. (1) yields an increase in radius of only

[a]Electronic mail: aarons@mit.edu.

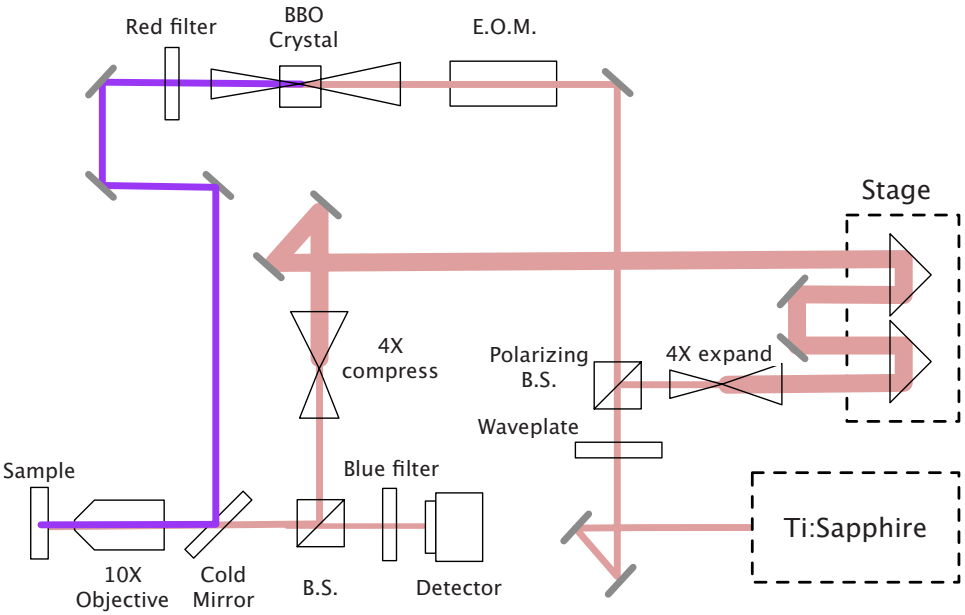

FIG. 1. (Color online) A schematic of the key elements of our pump-probe system. After the first beam splitter, the probe beam passes through a 4× beam expander to minimize divergence over 2 m (~7 ns) of delay, after which it is compressed before being directed onto the sample through an objective lens at normal incidence. The pump beam passes through an EOM and then a BBO crystal where it is frequency doubled to 400 nm. The doubled light is directed through the same objective lens onto the sample, coaxial with the probe beam.

0.02%. Measurement of the probe spot with a knife-edge profiler showed no perceptible change in size and a lateral shift of less than 0.5 μm over 7 ns of delay. Compared to the option of using an optical fiber after the stage to maintain beam shape,[10] the expander has the advantage that the probe power remains constant over the delay, eliminating the need for a normalizing detector. After the stage, the probe beam is compressed and directed through the center of a 10× objective at normal incidence. Changing the ratio of the compressor to the expander allows us to adjust the focused probe size by changing the diameter of the collimated probe beam into the objective lens.

The pump beam is passed through an electro-optic modulator (EOM) that modulates the beam at a frequency between 1 and 10 MHz. The modulation frequency serves as the reference for a lock-in amplifier which extracts the thermal signal from the background. After the EOM, a piece of beta-barium borate (BBO) crystal is used to double the frequency, producing light with a wavelength of 400 nm. Doubling the frequency of the pump beam has the significant advantage over single-color systems that it is easy to use dielectric mirrors and color filters to isolate the pump beam from the detector. This also allows us to use a simple coaxial geometry where pump and probe beams go through the center of the same objective lens, simplifying alignment and producing less distorted Gaussian spots. The color filters also allow us to measure relatively rough samples since the filters are not affected by scattering of the pump into different polarizations and angles. A pair of lenses focuses the pump beam onto the BBO crystal and recollimates it; by adjusting the distance between the lenses, we change the divergence of the beam and therefore the size of the focused pump spot. Typically we use a pump spot size with a $1/e^2$ radius of 25–30 μm and a probe spot with a radius of 4 μm to minimize any possible error due to probe beam walk off.

Liquid samples are held in the setup shown in Fig. 2. A piece of glass is coated with 60–100 nm of Al, which has a high thermoreflectance coefficient at 800 nm and acts a temperature transducer. Liquid is placed in contact with Al and is held in place with a second piece of glass. The second piece of glass typically has a channel 100–200 μm deep etched in it to contain the liquid, although in practice we achieve identical results if a flat piece of glass is used to trap a thin liquid layer with surface tension. The pump and probe beams impinge through the glass onto Al, and the properties of the liquid are deduced from the cooling curve. The same approach works for amorphous solids such as pastes, greases, and epoxies, which are simply applied to the Al surface.

III. THEORY

The output of the lock-in amplifier is given by[11]

$$Z = \frac{\beta Q}{T^2} \sum_{m=-\infty}^{\infty} H(\omega_0 + m2\pi/T) e^{im2\pi\tau/T}. \quad (2)$$

Here Q is the energy per pump pulse, T is the time between pulses, H is the frequency response of the sample, τ is the delay time between pump and probe pulses, and ω_0 is the pump beam modulation frequency. β is a constant account-

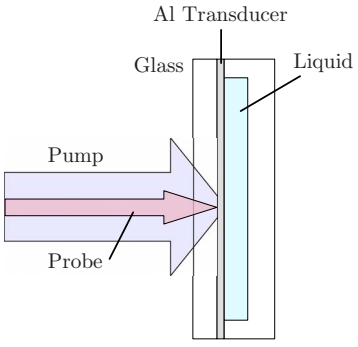

FIG. 2. (Color online) Sample arrangement for the measurement of liquid thermal properties. Liquid is placed on a slide coated with 60–100 nm of Al. A second piece of glass is used to contain the liquid. Typically the second piece of glass had a 100 μm etched channel to contain the liquid, but identical results were obtained if a flat piece of glass were used.

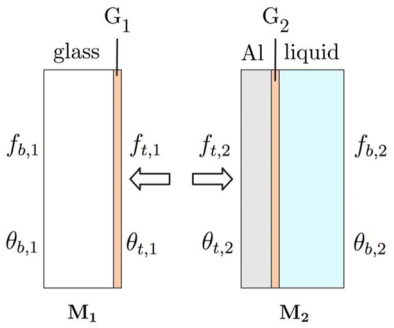

FIG. 3. (Color online) Thermal model for bidirectional heat conduction into the liquid and glass substrate. The problem is divided into two multilayer stacks: stack 1 consists of the thermal conductance between the glass and the Al transducer layer and a semi-infinite layer of glass; stack 2 consists of the Al transducer, the thermal conductance between the Al and the liquid, and a semi-infinite liquid layer.

ing for the thermoreflectance coefficient of the surface and the gain of the electronics. Equation (2) accounts for the accumulation effects of multiple laser pulses. When the time between pulses is long enough for the sample to return to its original state, Eq. (2) reduces to the inverse Fourier transform of the frequency response of the thermal system, i.e., the response to an impulse of heat with strength Q.

The thermal frequency response of the sample, $H(\omega)$, can be found by extending the solution of one-dimensional heat flow through a multilayer stack. For a single slab of material, in the frequency domain the temperature θ_t and heat flux f_t on the top side of the slab are related to the temperature θ_b and heat flux f_b on the bottom side through[14]

$$\begin{bmatrix} \theta_b \\ f_b \end{bmatrix} = \begin{bmatrix} \cosh(qd) & \frac{-1}{\sigma_z q}\sinh(qd) \\ -\sigma_z q \sinh(qd) & \cosh(qd) \end{bmatrix} \begin{bmatrix} \theta_t \\ f_t \end{bmatrix}. \tag{3}$$

Here d is the layer thickness, σ_z is the cross-plane thermal conductivity, and $q^2 = i\omega/\alpha$, where α is the thermal diffusivity.

For the case of unidirectional heat flow with a heat flux imposed on the top surface, multiple layers are handled by multiplying the matrices for individual layers together,

$$\begin{bmatrix} \theta_b \\ f_b \end{bmatrix} = \mathbf{M}_n \mathbf{M}_{n-1} \cdots \mathbf{M}_1 = \begin{bmatrix} A & B \\ C & D \end{bmatrix} \begin{bmatrix} \theta_t \\ f_t \end{bmatrix}, \tag{4}$$

where $\mathbf{M}_n$ is the matrix for the bottom layer. An interface conductance G is treated by taking the limit as the heat capacity of a layer approaches zero and choosing σ_z and d such that $G = \sigma_{z/d}$. If the nth layer is assumed to be semi-infinite, then the surface temperature will be given by

$$\theta_t = \frac{-D}{C} f_t. \tag{5}$$

We extend Eq. (4) to the case of bidirectional heat flow by solving two layered systems and matching the boundary conditions at the interface. The model is illustrated in Fig. 3. The first system, $\mathbf{M}_1$, is a two-layer stack consisting of the interface conductance G_1 between the glass slide and the Al and a semi-infinite glass layer. The second system, $\mathbf{M}_2$, has three layers: the Al layer, the conductance G_2 between the Al and the liquid, and a semi-infinite liquid layer. The boundary conditions at the interface are

$$\theta = \theta_{t,1} = \theta_{t,2}, \tag{6}$$

$$f = f_{t,1} + f_{t,2}, \tag{7}$$

where f is the total heat flux supplied to the system. After some algebra, we find the temperature of the Al layer at the Al-glass interface,

$$\theta = \left(\frac{-D_1 D_2}{C_1 C_2 + D_2 C_1} \right) f, \tag{8}$$

where C_1, D_1 and C_2, D_2 are the matrix elements from Eq. (4) that correspond to systems 1 and 2, respectively. The interface temperature θ is the quantity measured in the experiment and corresponds to H in Eq. (2).

Equation (8) can be extended including the effects of radial conduction caused by finite laser spot sizes. The problem has cylindrical symmetry, so a zero-order Hankel transform can be used to simplify the equations. The Hankel transform of $\theta(r)$ is given by.[14]

$$H_0[\theta(r)] = \int_0^\infty r J_0(kr)\theta(r) dr, \tag{9}$$

where k is the transform variable and r is the radial coordinate. Applying the transform to the governing diffusion equation and repeating the procedure described in Eqs. (3)–(8) yields identical results, except that now q in Eq. (3) is given by

$$q^2 = \frac{\sigma_r k^2 + \rho c i\omega}{\sigma_z}, \tag{10}$$

where σ_r and σ_z are the radial and cross-plane thermal conductivities, respectively, ρ is the density of the layer, c_p is the specific heat, and k is the transform variable. The heat flux term f at the boundary is given by the Hankel transform of a Gaussian spot with power A_0 and $1/e^2$ radius w_0. The interface temperature from Eq. (8) then becomes

$$f = \left(\frac{-D_1 D_2}{D_1 C_2 + D_2 C_1} \right) \frac{A_0}{2\pi} \exp\left(\frac{-k^2 w_0^2}{8} \right). \tag{11}$$

This result is still in the transform domain. To find frequency response H in real space, we must take the inverse Hankel transform and then weight the result by the probe intensity distribution, which is taken as a Gaussian spot with $1/e^2$ radius w_1,[11]

$$H(\omega) = \frac{A_0}{2\pi} \int_0^\infty k \left(\frac{-D_1 D_2}{D_1 C_2 + D_2 C_1} \right) \exp\left[\frac{-k^2 (w_0^2 + w_1^2)}{8} \right] dk. \tag{12}$$

This solution for the frequency response is inserted in Eq. (2), which we solve numerically.

In order to extract the liquid thermal conductivity k, we use a least-squares minimization routine to vary the liquid thermal conductivity k and the Al-liquid interface conductance, G_2, to match the phase of Eq. (2) to the data. The sensitivity of the measurement is limited by heat flow into

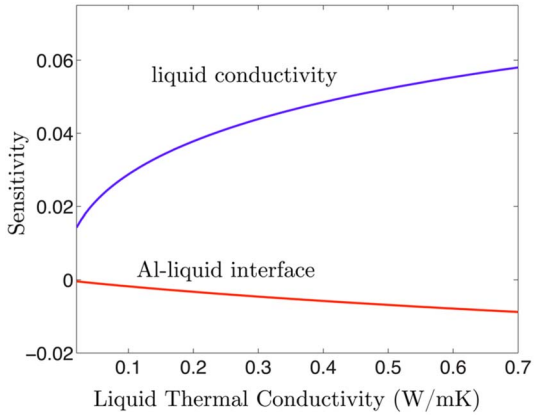

FIG. 4. (Color online) Sensitivity to the liquid thermal conductivity (upper figure) and the aluminum-liquid thermal interface conductance (lower figure) taken at a delay time of 1000 ps, plotted as a function of liquid thermal conductivity.

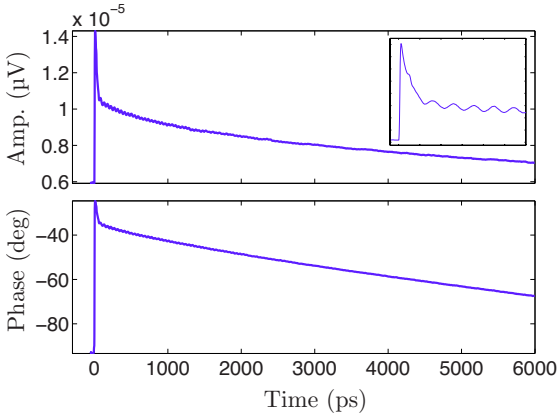

FIG. 5. (Color online) Amplitude and phase of a typical signal obtained from the lock-in amplifier during a measurement (in this case decane). The inset shows the first 300 ps, which show clearly the signal oscillations due to Brillouin backscattering.

the glass, which has a thermal conductivity on the order of 1 W/m K; sensitivity increases as the fraction of heat flowing into the liquid increases. We take the sensitivity of our measurement to a parameter x as the logarithmic derivative $S_x = d\,\phi / d\ln x$, where ϕ is the phase angle. Figure 4 shows the sensitivity to the liquid thermal conductivity and the Al-liquid conductance as a function of liquid thermal conductivity. The values are plotted for a delay time τ of 1000 ps, although the curves look similar over the range of delay times. As the figure shows, the model is one to two orders of magnitude more sensitive to the liquid thermal conductivity than the interface conductance.

IV. RESULTS AND DISCUSSION

Values for the thermal conductivity of the glass slide and the glass-Al thermal conductance G_1 were obtained by performing a pump-probe measurement on the Al-coated side. The aluminum thickness was determined to within 2 nm via the acoustic echoes of the thermal shock wave.[15] The glass thermal conductivity was found to be 1.12 W/m K and the interface conductance was approximately 150 MW/m^2 K. These values were kept constant in all subsequent fitting of liquid properties.

The amplitude and phase of a typical signal obtained from the lock-in amplifier during a measurement of decane are shown in Fig. 5. The damped oscillations are due to Brillouin backscattering in the glass slide.[16] The acoustic frequency $f_{ac}=21$ GHz is related to the probe wavelength through $f_{ac}=2nc/\lambda$, where n is the index of refraction and c is the speed of sound in the glass. The oscillations are small enough compared to the thermal signal that they do not interfere with the model fit.

Either the amplitude or phase data can be compared to Eq. (2) to extract the liquid thermal conductivity. In practice, we find that fitting to the phase produces more reliable results because it is slightly less noisy and removes any difficulties associated with normalization. As mentioned above, we use a least-squares minimization routine to vary k and G_2 to match Eq. (2) to the data. The fit value for the interface conductance varied widely at different locations on the sample, and from liquid to liquid. We attribute this to the fact that our slides became microscopically scratched after numerous tests and also to the fact that the model is generally not very sensitive to the interface parameter, as shown in Fig. 4. Nonetheless, values for G_2 typically ranged from 50 to 100 MW/m^2 K for our samples, in fair agreement with other findings.[7] Sample data and best fit curves for four liquids are shown in Fig. 6.

Six liquids and a thick silicone grease were measured with this method at room temperature. Typically, we would measure five locations on a sample and take the mean value; variation between locations was on the order of 10%, slightly higher for the low conductivity liquids. The results are compared to the accepted values at 300 K in Fig. 7. The largest error is less than 5%.

Two potential sources of error that should be examined are the effects of convection and the steady temperature rise of the sample due to prolonged heating. We verified that convection was not present by trying three liquid channel depths (200 μm, 100 μm, and a droplet squeezed between two slides) for two liquids, water and decane. One would

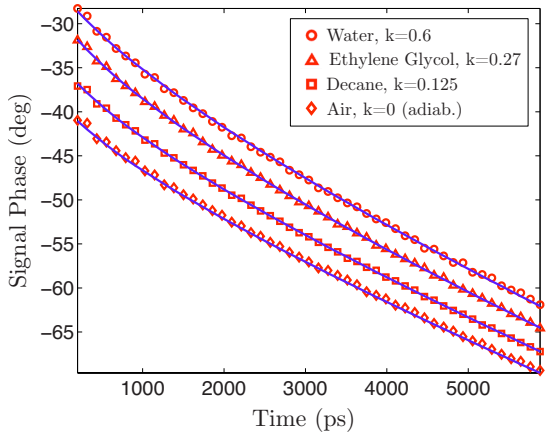

FIG. 6. (Color online) Phase data and best fit curves for four fluids: water, ethylene glycol, decane, and air. Fit values for thermal conductivity are indicated in W/m K. The fit for air was obtained by setting the fluid thermal conductivity to zero and represents the lower bound on measurable liquid thermal conductivity.

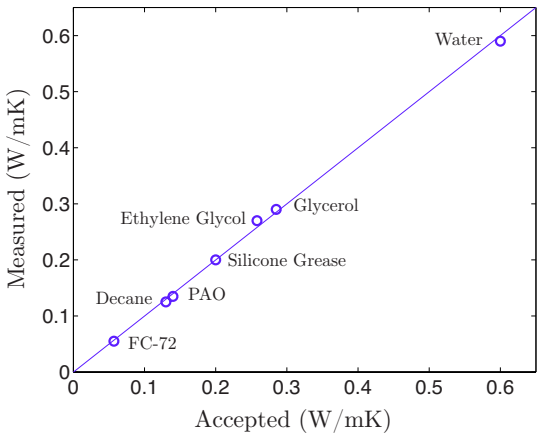

FIG. 7. (Color online) Thermal conductivity results at 300 K obtained for six liquids and silicone grease. Each data point represents the the average of several measurements (usually 5) taken at different locations on the sample; variation between locations was on the order of 10%.

expect that viscous forces would overwhelm inertial forces at these length scales, and indeed we saw no change in our results among these configurations. The steady temperature rise can be estimated by taking the low frequency limit of Eq. (12).[11] We consider only the temperature rise in the glass; this will be an upper bound estimate on the temperature rise,

$$\Delta T = \frac{(1-R)\dot{q}}{\sigma(2\pi w_0^2 + 2\pi w_1^2)^{1/2}}. \tag{13}$$

Here ΔT is the steady temperature rise, $\dot{q}$ is the incoming laser power, R is the sample reflectivity, σ is the thermal conductivity, and w_0 and w_1 are the pump and probe radii, respectively. For our typical pump power of 25–40 mW over a $1/e^2$ diameter of 50 μm and a reflectivity of around 0.9–0.95, we estimate a steady rise of 10–20 K. We did not see a significant change in our results as we changed the pump power from 20 to 80 mW, although above 80 mW signal stability decreased, possibly due to bubble formation.

V. SUMMARY

We have introduced a convenient optical technique for measuring the thermal conductivity of liquids. Pump-probe systems are becoming commonplace in universities and research laboratories. Now, with an Al-coated glass slide, these systems can rapidly measure a wide variety of liquids. The technique is immune to convective effects and can measure extremely small volumes. Although there is likely a steady heating effect of 10–20 K, the sample could be placed in a temperature controlled environment with an optical window and temperature-dependent thermal conductivity measurements could be made. Doing this for a well-characterized liquid would reveal the nature of the steady offset.

ACKNOWLEDGMENTS

The authors would like to thank Professor David Cahill and Xuan Zheng of the University of Illinois at Urbana-Champaign and Professor Keith A. Nelson, Darius H. Torchinsky, and Christoph Klieber of MIT for their many helpful discussions. This work was partially supported by the Ford-MIT Alliance, the Norwegian Research Council, and an NSF Graduate Research Fellowship for A. Schmidt.

[1] S. D. Brorson, A. Kazeroonian, J. S. Moodera, D. W. Face, T. K. Cheng, E. P. Ippen, M. S. Dresselhaus, and G. Dresselhaus, Phys. Rev. Lett. **64**, 2172 (1990).
[2] T. Q. Qiu and C. L. Tien, Int. J. Heat Mass Transfer **35**, 719 (1992).
[3] W. S. Capinski, H. J. Maris, T. Ruf, M. Cardona, K. Ploog, and D. S. Katzer, Phys. Rev. B **59**, 8105 (1999).
[4] S. Huxtable, D. G. Cahill, V. Fauconnier, J. O. White, and J.-C. Zhao, Nat. Mater. **3**, 298 (2004).
[5] R. J. Stoner and H. J. Maris, Phys. Rev. B **48**, 16373 (1993).
[6] B. C. Gundrum, D. G. Cahill, and R. S. Averback, Phys. Rev. B **72**, 245426 (2005).
[7] Z. Ge, D. G. Cahill, and P. V. Braun, Phys. Rev. Lett. **96**, 186101 (2006).
[8] Z. Ge, D. Cahill, and P. Braun, J. Phys. Chem. B **108**, 18870 (2004).
[9] H. Eichler, Opt. Acta **24**, 631 (1977).
[10] W. S. Capinski and H. J. Maris, Rev. Sci. Instrum. **67**, 2720 (1996).
[11] D. G. Cahill, Rev. Sci. Instrum. **75**, 5119 (2004).
[12] Y. Nagasaka and A. Nagashima, J. Phys. E **14**, 1435 (1981).
[13] E. Hecht, *Optics* (Addison-Wesley, New York, 1997).
[14] H. S. Carslaw and J. C. Jaeger, *Conduction of Heat in Solids* (Oxford University Press, New York, 1959), pp. 109–112.
[15] G. Tas and H. J. Maris, Phys. Rev. B **49**, 15046 (1994).
[16] N. Ashcroft and D. Mermin, *Solid State Physics* (Holt Rhinehart, New York, 1976).